[Rock and Soil Mechanics](https://rocksoilmech.researchcommons.org/journal)

Volume 41 | Issue 12 Article 8

4-29-2021

Mechanism research of a new constant resistance yielding device for tunnels

Chuan-qing ZHANG
State Key Laboratory of Geomechanics and Geotechnical Engineering, Institute of Rock and Soil Mechanics, Chinese Academy of Sciences, Wuhan, Hubei 430071, China

Hao-an L
University of Chinese Academy of Sciences, Beijing 100049, China

Xiao-yan LIU
University of Chinese Academy of Sciences, Beijing 100049, China

Hui ZHOU
State Key Laboratory of Geomechanics and Geotechnical Engineering, Institute of Rock and Soil Mechanics, Chinese Academy of Sciences, Wuhan, Hubei 430071, China

See next page for additional authors

Custom Citation

ZHANG Chuan-qing, LÜ Hao-an, LIU Xiao-yan, ZHOU Hui, GAO Yang, YAN Dong-ming, . Mechanism research of a new constant resistance yielding device for tunnels[J]. Rock and Soil Mechanics, 2020, 41(12): 4045-4053.

Rock and Soil Mechanics 2020 41(12): 4045−4053 ISSN 1000−7598
https: //doi.org/10.16285/j.rsm.2020.5436 rocksoilmech.researchcommons.org/journal

Mechanism research of a new constant resistance yielding device for tunnels

ZHANG Chuan-qing[1], LÜ Hao-an[1, 2], LIU Xiao-yan[1, 2], ZHOU Hui[1], GAO Yang[1], YAN Dong-ming[3]

1. State Key Laboratory of Geomechanics and Geotechnical Engineering, Institute of Rock and Soil Mechanics, Chinese Academy of Sciences, Wuhan, Hubei 430071, China
2. University of Chinese Academy of Sciences, Beijing 100049, China
3. College of Civil Engineering and Architecture, Zhejiang University, Hangzhou, Zhejiang 310058, China

Abstract: The constant resistance yielding support is the ideal form of support for squeezing tunnel. Current technology is difficult to satisfy the safety requirements of high bearing capacity, large deformation and load stability at the same time. In response to this problem, the constant resistance yielding device based on the principle of tension-compression conversion (CRYD-TCC) was developed inspired by the metal drawing process in combination with the working characteristics of steel arch support. In this paper, the working principle of the CRYD-TCC was discussed, and its mechanical response law and characteristics were analyzed. Through the indoor test and numerical simulation, the influence of the design parameters was analyzed, and the performance measurement index of the CRYD-TCC was determined. The analysis shows that: 1) The CRYD-TCC can constantly resist deformation under pressure; when installed in the steel arch joint allowing it to be part of the steel arch, the device can ensure the stability of the arch, improve its large deformation adaptability while providing constant support for the surrounding rock. 2) Based on the four design parameters: the cone angle, the friction coefficient, the cross-section shrinkage rate and the diameter of the pressure bar, the device can realize pressure resistance and pressure control with satisfactory load stability, which can provide important technical support for soft-rock tunnel large deformation and the stability control of support.

Keywords: yielding support; squeezing large deformation; constant resistance yielding device; numerical simulation

1 Introduction

With the continuous development of infrastructure construction in China including water conservancy and hydropower, railways, and highways, tunnel engineering projects continue to merge in high-in-situ soft rock ground setting. For example, the Sichuan−Tibet Railway and the Central Yunnan Water Diversion Project both will inevitably pass through soft rock formations, where large deformations are a major challenge in the construction of these tunnels (caverns). When the surrounding rock undergoes large deformation, huge pressure will be generated and acts upon the shotcrete layer, steel arch frame and other supporting structures, resulting in bulging and rupture of the shotcrete layer, twisting and instability of the steel arch frame, and anchor rod breakage. At present, when domestic tunnels (caverns) encounter large deformation due to squeezing, rigid support schemes such as increasing the shotcrete thickness and increasing the density or stiffness of steel arches are often adopted[1]. However, because the rigid support only allows for small deformation and is limited in bearing capacity, it cannot effectively control the deformation of the surrounding rock after premature failure.

Since the 20th century, there have been different opinions on the mechanism and causes of large compression deformation, both domestic and international scholars, however, reached a consensus: with the surrounding rock continues to deform, the stress released by surrounding rock is gradually reduced. Therefore, in a hope to prevent the support from premature failure, the concept of flexible yielding that allows the squeezing ground to deform by a certain amount, in combination with the theoretical and technological principles of this support innovation, has achieved significant development. For example, Kovári et al.[2] proposed to fill the compressible material between the outer wall of the rigid support and the surrounding rock to allow the surrounding rock to produce a certain-degree of convergent deformation while ensuring that the tunnel section remains largely unchanged. Anagnostou et al.[3] modified the structure of the steel arch or shotcrete layer that allows it to have the pressure relief function, such as installing a steel arch support with sliding function (such as a retractable U-shaped steel arch) or installing compressible structure in a steel arch and the shotcrete support section. Hoek et al.[4] divided the steel arch into several sections, and installed two sliding structures at the segment joints, the friction of the joints thus functioning as pressure relief at the steel arch. Thut et al.[5] placed high deformable concrete (HDC) with high compressibility and certain strength in the reserved groove for lining. This helped prevent damage to the lining due to overly strong rigidity. Schubert et al.[6] installed lining stress controllers (LSC) in the reserved grooves of the lining

Received: 16 April 2020 Revised: 10 August 2020
This work was supported by the Yalong River Joint Fund of the National Natural Science Foundation of China(U1865203), the National Natural Science Foundation of China(51709257) and the Hubei Province Natural Science Foundation Innovation Group(2018CFA013).
First author: ZHANG Chuan-qing, male, born in 1977, PhD, Professor, PhD supervisor, mainly engaged in research on deep rock mechanics and deep disaster prevention. E-mail: cqzhang@whrsm.ac.cn
Corresponding author: LÜ Hao-an, male, born in 1996, Postgraduate, majoring in underground engineering support and numerical calculation. E-mail: lvhaoan@163.com

and steel arch, which significantly improved the safety of the support. In recent years, many Chinese scholars have conducted related researches. He et al.[7] developed a large-deformation anchor structure of constant resistance and negative Poisson's ratio. The principle is that the inner cone of the anchor slips to allow the casing to expand radially, thus resulting in constant resistance. Academician Sun et al.[8] proposed a large-scale yielding anchor and a prestressed anchor cable, which provides support from the compression force and dynamic frictional resistance generated by the relative sliding of the extrusion head in the sleeve. Chen et al.[9] used foam concrete as the filling material for the deformation layer between the primary support and the secondary lining, which helped to relieve the creep deformation pressure of the lining. Pan et al.[10] developed a wave energy-absorbing buffer device, which effectively solved the problem of rock bursts in coal mine roadways by using metal foam in the curved shell and ribbed pipe. Lei et al.[11] designed a metal buckling pressure relief device, which used the rigidity-flexibility-rigidity characteristics of the pressure relief device during the loading process to achieve pressure dissipation. Tang et al.[12] designed an energy-absorbing and anti-impact component with radial expansion. The thin-walled round tube was deformed by constant resistance expansion through the moulding motion, which improved the stress condition of the column under loading. Qiu et al.[13] developed a limiter that solved the problem of primary support cracking of deep-buried loess tunnels through the process of steel slab yielding, bending and compaction.

Constant resistance yielding support is an ideal support form in the adaptation and control of large deformation of tunnels in squeezing ground. With the adjustment to the stress in the surrounding rock, the load acting on the support increases, and the pressure relief function is triggered once the designed resistance value is met. The rock and the support deform together and gradually tend to converge. At present, all kinds of flexible yielding support have achieved certain effects in controlling the large deformation of tunnels (caverns). However, the existing technology is still unable to simultaneously meet the requirements of high bearing capacity, large deformation controlling and stable loading. Steel arch is an important structure in the tunnel (cavern) support system, which is essential to maintain the initial stability and control the development of deformation. However, the friction force of the existing yielding sliding friction type yielding structure is unstable and greatly affected by the construction quality. In other words, the compressible yielding structures generally have unstable bearing capacity during the compression process, and are prone to instability and damage.

Because of the aforementioned limitations, a new type of constant resistance yielding device (CRYD-TCC) based on the principle of tension-compression conversion was developed in this study. It is capable of converting between tension and compression. The device is installed at the joint of the steel arch frame, which allows the simultaneous deformation of the steel arch frame and the surrounding rock. It provides the surrounding rock with a constant support during its deformation. In addition, both the support resistance and the range of yielding deformation can be adjusted by the design parameters. Based on the principle of constant resistance and yielding deformation, this paper analyses the device's mechanical response and characteristic properties. Through indoor tests and numerical simulations, the feasibility of the device is verified, and the influence of various design parameters is discussed so as to promotes the future application of this supporting structure.

2 Principle of constant resistance and yielding deformation

Under high stress conditions, the excavation of tunnels (caverns) in weak rock will cause a long-lasting extrusion and large deformation. The ISRM (International Society of Rock Mechanics and Rock Engineering) defines the compressibility of surrounding rock as the large deformation of the surrounding rock with time, which is essentially the shear creep caused by the overstress in the rock body. The deformation can occur during the construction phase, and may last a long time[14]. During the construction of a soft rock tunnel (cavern), rigid supports can only temporarily control the deformation of the surrounding rock. The allowable displacement of these supports is very limited. Along with time, the energy restored in the rock cannot be released, and would eventually acts on the support, causing it to be damaged. Therefore, before the application of ultra-high strength support materials or ultra-high bearing capacity support systems, the support depending strongly on rigidity should not be considered when coming to tunnel (cavern) design in squeezing ground.

With the development of the New Austrian Tunnelling Method and the proposed convergence-constraint calculation method, the idea of combining support and yielding deformation for tunnelling under condition of high ground stress and large deformation has been acknowledged based on the surrounding rock characteristic curve shown in Fig. 1[15]. While making full use of the self-supporting capacity of the surrounding rock, the surrounding rock is deformed under a constant resistance condition through constant resistance yielding support. A part of the energy in the rock body is released by pressure reduction, while the support provided via the constant resistance controls the deformation of the surrounding rock within a safe range. Under the combined action of the surrounding rock and the support, the plastic-zone development of the surrounding rock is controlled and the stability of the surrounding rock is maintained.

3 Design of CRYD-TCC

Similar to the cold-drawing process of metal materials,

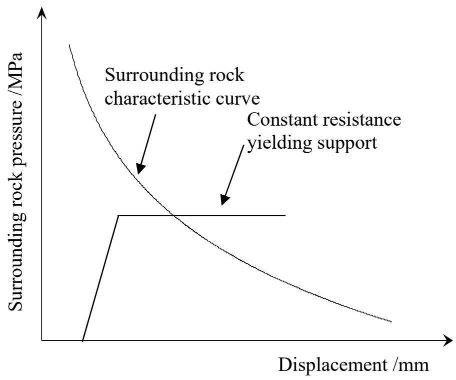

Fig. 1 Convergence–confinement curve for surrounding rock[15]

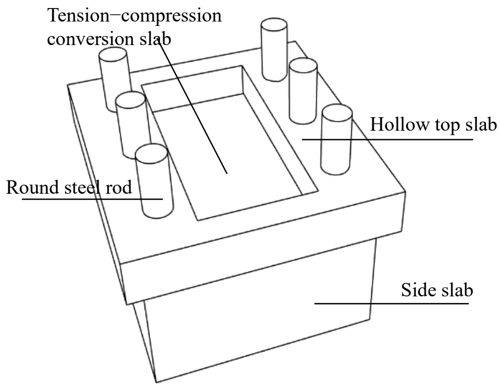

Fig. 2 Structure of CRYD-TCC

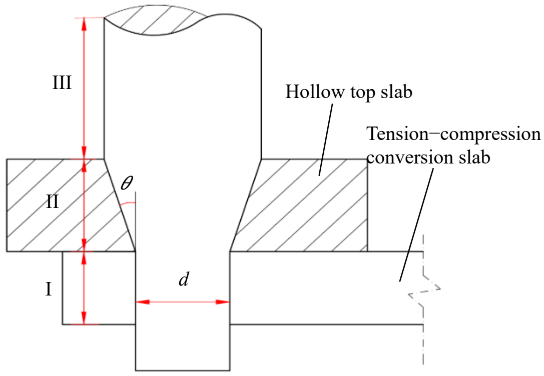

Fig. 3 Device details

Charette et al.[16] proposed the Roofex® anchor rods, Varden et al.[17] designed the Garford dynamic anchor rods, and Wang et al.[18] also proposed a similar anchor rod that has similar working principle as cold-drawing. The main rod is consisted of two sections with different diameters, and a bushing is arranged in the transition area. As the surrounding rock deforms, the rod is stretched. Because the diameter of the bushing die hole is smaller than that of the wide rod section, the rod would be deformed plastically and the thinner rod would be slowly pulled out.

Based on the working principle of this anchor rod, a constant resistance yielding device based on the principle of tension-compression conversion (CRYD-TCC) is designed and introduced in this paper that considered the structural force characteristics of the steel arch support, and applied tension members to the compression structure.

3.1 The structure of the tension-compression conversion

As shown in Fig. 2, the CRYD-TCC consists of the tension–compression conversion slab, round steel rods, side slabs and a hollow top slab with tapered holes. Some details of the device are shown in Fig. 3. The round steel rod is divided into 3 rod sections. The first section passes through the cone hole of the top slab and is fixedly connected to the tension-compression conversion slab; the taper of the second rod section is consistent with the cone hole of the hollow top slab; The third section is located on the hollow top slab, and the diameter of the third section is larger than that of the first section. The round steel rods are arranged symmetrically on two sides of the hollow top slab, and the number of rods can be adjusted according to actual engineering conditions.

3.2 The working principle of CRYD-TCC

The working principle of the CRYD-TCC is shown in Fig. 4. The end of the steel arch node passes through the hollow top slab to directly act on the tension–compression conversion slab to generate a vertical pressure *P*. The slab then converts the vertical pressure *P* into a tension on the round steel rob. As the surrounding rock of the tunnel deforms, the internal force of the steel arch frame increases, and then the vertical pressure *P* increases. The pulling force acting on the first section of the round steel rob increases, because the diameter of the third section of the round steel rod is larger than that of the first section. When the tension increases to a certain degree, the second rod section of the round steel rod will overcome the resistance of the cone hole to produce shrinkage deformation, the second rod section will become thinner and gradually pass through the cone hole of the top slab, and at the same time the conversion slab also moves downwards, so as to realize the constant resistance and pressure reduction of the steel arch support.

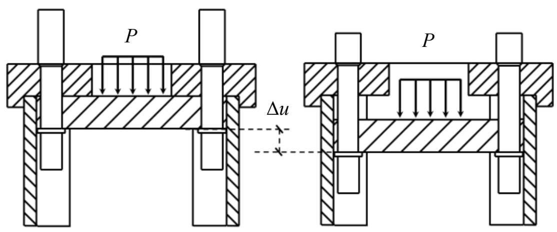

Fig. 4 Work process of CRYD-TCC

The placement of CRYD-TCCs on steel arch in section view for actual engineering use is shown in Fig. 5. As the surrounding rock converges, the pressure acting on the steel arch frame gradually increases. When it reaches the design value, the CRYD-TCC is triggered, and the device generates yielding deformation. As each device is triggered, the overall circumference of the steel arch frame is reduced, and the steel arch frame moves inwards creating a displacement of s in the radial direction ($2\pi s = n\Delta u$, n is the number of the devices being installed).

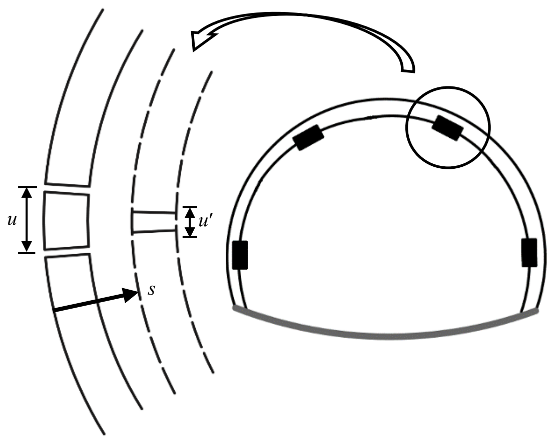

Fig. 5 Yielding principle of steel arch

3.3 Applicable conditions of CRYD-TCC

The design of the CRYD-TCC needs to meet two requirements that state: (1) when the second section of the round steel rod is forced to yield with shrinkage and deformation, the internal tensile stress of the rod should not be greater than the tensile strength of the round steel rod material, otherwise the first section will yield or even break directly; and (2) the constant resistance of the support provided by the CRYD-TCC should be less than the load-bearing capacity of the steel arch frame, otherwise it may cause the steel arch frame to fail before the device takes effect, resulting in failure of pressure reduction.

In engineering field application, the yielding devices should be arranged considering the stress distribution of the surrounding rock of the tunnel. Design optimization should be carried out that analyzes the instability mode and position of the steel arch. In addition, tests should be performed to make sure that the yielding devices can operate normally under axial pressure. It should be avoided to install the devices at places with stress concentration or large local deformation. Figure 6 shows the two basic working forms of the devices.

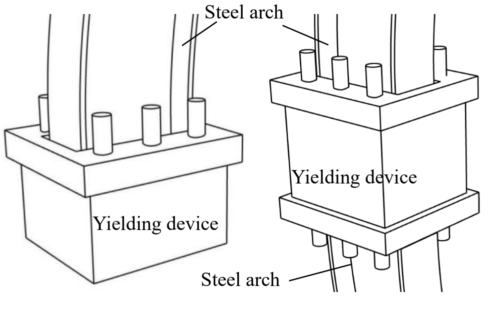

Fig. 6 Work forms of CRYD-TCC

4 Mechanical response test of CRYD-TCC

In order to study the mechanical response of the CRYD-TCC at work, a small device that can be used for indoor tests was processed, as shown in Fig. 7. The overall size of the device is 210 mm×150 mm×180 mm, and the square hole size of the hollow top slab is 100 mm×100 mm. The surrounding side slabs, the tension−compression conversion slab and the hollow top slab are all made with #45 steel. Considering that the tension−compression conversion slab will be directly subjected to pressure, the material used to build the slab has therefore been heat treated to improve its physical properties. In order to facilitate the development of the test, a bushing with a tapered hole inside was specially processed to replace the role of the tapered hole in the hollow top slab. The tapered hole in the processed bushing has a diameter of 11.5 mm, an outlet diameter of 10 mm, and a cone angle of 2.6º. Because the round steel rod is plastically deformed in the tapered hole of the bushing, the hardness of rod therefore should be lower than that of the bushing and should have better ductility, while ensuring that the two materials have a smaller coefficient of friction. Based on the investigation of various types of steel, this paper selects the heat-treated Cr12MoV industrial die steel as the bushing material, and the Q235 steel as the pressure bar material.

The test was carried out on a 600 kN hydraulic uniaxial loading test machine. A manual pump was used to pressurize the device, the hydraulic instrument panel and the electronic dialgage were employed to record the real-time loading and the real-time yielding displacement, respectively. In order to reduce the friction between the round steel rod and the bushing, lubrication treatment is also carried out.

Fig. 7 CRYD-TCC with bushing

The load−displacement curve obtained from the test is shown in Fig. 8. It can be seen that the load−displacement curve can be divided into three stages: the first stage is associated with elastic deformation. As the load increased, the round steel rod was brought into close contact with the inner wall of the bushing, and became elastically deformed under tension; the second stage is associated with nonlinear deformation. Due to the tapered inner wall of the bushing, the round steel rod was subjected to an annular pressure and friction, and the metal material began to plastically deform and squeeze upward, and the deformation continued nonlinearly; the third stage is the stable deformation stage. With further deformation, the deformation of the metal inside the pressure bar became stabilized, and the metal continued to plastically deformed and squeezed upwards. While the load remains almost unchanged, the displacement continued to increase. When the round steel rod was slowly pulled out, the entire device entered a quasi-static process. Given no consideration to the influence of the frictional heating, material strengthening and other factors, the device is capable of providing constant resistance. Figure 9 shows the change of the CRYD-TCC before and after the test.

Analysis of the test curve suggests that there are two indicators for evaluating the device's performance, which are the constant resistance and the allowable yielding deformation.

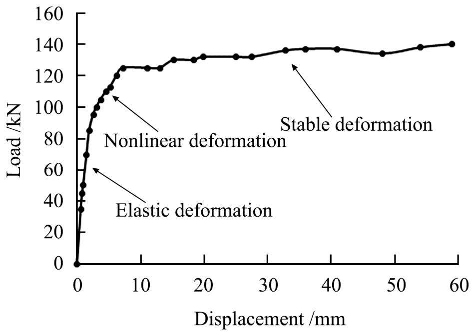

Fig. 8 Loading−displacement curve of CRYD-TCC

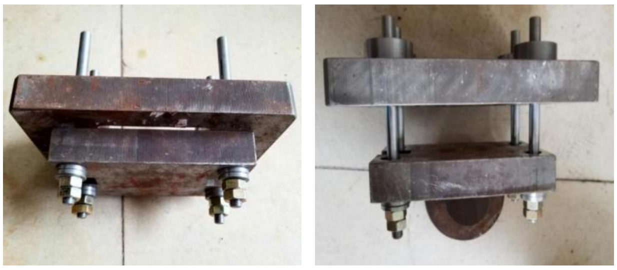

(a) Before test (b) After test

Fig. 9 CRYD-TCC before and after the experiment

Based on NATM, in order for the pressure support system to better exert the self-supporting capacity of the surrounding rock, it is necessary to set a reasonable constant resistance and allowable yielding deformation. If the constant resistance is set too low or the allowable yielding deformation set too large, it may cause loose damage or collapse of the rock mass due to excessive deformation of the surrounding rock; if the pressure resistance is set too high or the allowable yielding deformation is set too limited, the steel arch would still bear excessive pressure, and therefore not having an optimal yielding effect.

5 Simplification of analysis for force characteristics of the round steel rod

In order to explore the mechanical characteristics of the CRYD-TCC during yielding deformation, only a single round steel rod is selected as the research object. The analysis gives no consideration to the influence of the rod material defects, additional bending moment, and friction during the drawing process and temperature. In the process of yielding deformation, the rod is subjected to axial tension and compression in the other two directions, which has some similar characteristics as the problem of thick spherical shells under internal pressure[19]. Because the strain analysis of the thick spherical shell is based on small deformation, for large deformation problem that makes the compression rod to shrink and deform, the analysis in this section assumes that the device enters a stable deformation state when the strain state of the rod is kept unchanged. The material of round steel rod is an ideal elastic-plastic non-compressible material.

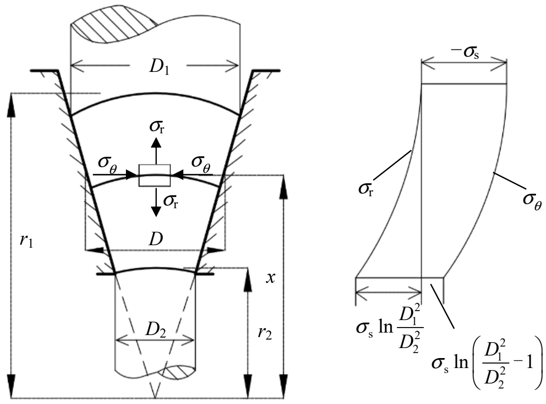

Fig. 10 Tensile stress state of yielding bar

The round steel rod in the cone hole is regarded as a part of the spherical shell whose outer radius is r_1, and the inner radius is r_2, and this part of the spherical shell is subjected to internal tension, as shown in Fig. 10. For a thick spherical shell subjected to internal pressure, the radial stress σ_r is always negative, and the circumferential stress σ_θ is always positive, then the first and second principal stresses are $\sigma_1 = \sigma_2 = \sigma_\theta$, and the third principal stress is $\sigma_3 = \sigma_r$, the Mises yield condition is the same as the Tresca yield condition, which is $\sigma_\theta - \sigma_r = \sigma_s$, σ_s is the yield strength. The principal stress state of the round steel rod (approximately regarded as a thick-walled spherical shell under internal tension) is

$$\left.\begin{aligned}\sigma_1 = \sigma_2 = \sigma_r \\ \sigma_3 = \sigma_\theta\end{aligned}\right\} \tag{1}$$

The Mises yield condition and Tresca yield condition are also the same as

$$\sigma_r - \sigma_\theta = \sigma_s \tag{2}$$

Incorporate Eq. (2) into the shell equilibrium differential equation:

$$\frac{d\sigma_r}{dr} - 2\frac{\sigma_\theta - \sigma_r}{r} = 0 \tag{3}$$

where r is the radius at any thickness.

By solving Eq. (3), the principle stresses are obtained as

$$\left.\begin{aligned}\sigma_r &= c-\sigma_s \ln r^2 \\ \sigma_\theta &= c-\sigma_s \ln(1+r^2)\end{aligned}\right\} \tag{4}$$

where c is the integral constant. The integral constant in Eq. (4) can be determined by the stress condition at the entrance of the cone hole, which are $r = r_1$, $\sigma_r = 0$. From which the integral constant can be obtained to be $c = \sigma_s \ln r_1^2$.

By introducing the diameter of the third section of the round steel rod D_1, the diameter of the first rod section D_2, and the diameter of any part of the second rod section D, we have $r_1/r = D_1/D$. Substituting $r_1/r = D_1/D$ into Eq. (4) results in the principle stressed as

$$\left.\begin{aligned}\sigma_r &= \sigma_s \ln \frac{D_1^2}{D^2} \\ \sigma_\theta &= \sigma_s \left(\ln \frac{D_1^2}{D^2} - 1\right)\end{aligned}\right\} \tag{5}$$

During the yielding process, the rod is subjected to the maximum compressive stress in the critical state of deformation and the maximum tensile stress at the exit of the cone hole. Radial stress always acts to reduce the surface area, so the farther from the rod, the larger the area of the outer surface and the greater the stress is required. According to the yield criterion, the closer to the surface of the rod, the greater the compressive stress, and the smaller the tensile stress; and the center of the rod experiences the smallest compressive stress and the greatest tensile stress. Therefore, the center of the rod is the most easily prone to breakage due to the small diameter. This conclusion should provide reference to the selection of rod material and size design of round steel rod.

6 Analysis of CRYD-TCC design parameters

The allowable constant resistance and yielding deformation of the CRYD-TCC should be designed according to actual engineering conditions. The allowable yielding deformation can be adjusted arbitrarily by changing the length of the third section of the round steel rod and the height of the side slab. The allowable constant resistance is mainly governed by the size and number of the round steel rod and the cone holes of the top plate.

Through the analysis of the plastic shrinkage deformation process of the round steel rod, four parameters are summarized that have the most prominent influence on the constant resistance of the rod: cone angle, friction coefficient, rod cross-sectional shrinkage rate (the ratio of the difference between the cross-sectional areas of the first and third section of the rod to the cross-sectional area of the third section), and diameter of the first rod section (hereinafter referred to as the diameter). This section uses the LS-DYNA module in ANSYS to calculate and systematically study their influence on constant resistance.

6.1 Calculation model

In order to facilitate the study of a single round steel rod, according to its actual size and the bushing used in the test as described in Section 5, a 1:1 calculation model was established, so that the diameter of the first section of the round steel rod is 10 mm, the diameter of the third rod section is 11.5 mm, and the cone angle is 2.6º, Figure 11 shows the calculation model and the meshing.

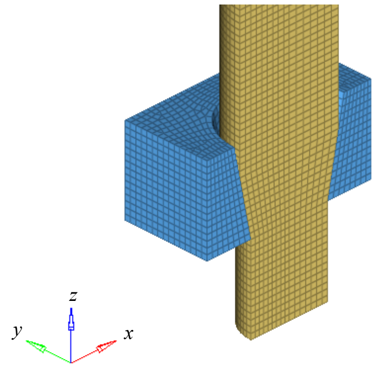

Fig. 11 1/2 yielding bar model

6.2 Material parameters

The actual material of the round steel rod is Q235, which has a Young's modulus of 206 GPa, a Poisson's ratio of 0.3, and a density of 7.9×103 kg/m^3. The input stress and strain data are shown in Table 1. The hollow top slab is actually an industrial die steel material. To ensure calculation efficiency, it is treated as a rigid body.

Table 1 Stress and strain data

Strain	0.001	0.01	0.02	0.03	0.05	0.10	0.20
Stress /MPa	240	245	250	300	380	455	460

6.3 Boundary conditions

The contact type of the round steel rod and the bushing was set to surface contact. The degrees of freedom of the bushing in the X-axis, Y-axis and Z-axis were constrained, and the degrees of freedom of the round steel rod in the X-axis and Y-axis were also constrained. The loading was applied at a constant speed of 1 mm/s on the lower end of the round steel rod.

6.4 Analysis of numerical simulation results

Figure 12 shows the comparison between the numerical calculation results and the test results. There were 4 round steel rods used during the test, and only one of them was simulated, so the simulation result was multiplied by 4. It can be seen that the load–displacement curve obtained from the simulation is basically consistent with the test results, but the test curve has showed a slow increasing trend, which may be the manifestation of the strengthening effect when the metal is deformed.

Figure 13 shows the stress distribution in the process of rod being deformed. It can be seen that the round steel rod inside the cone hole accumulates the highest stress, the stress of the outer elements is higher than that of the elements towards the center, indicating that the closer to the outer side of the round steel rod, the greater the stress

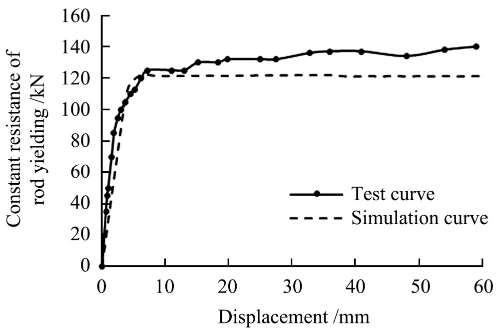

Fig. 12 Comparison between numerical results and measured data

required. This is because the material on the surface of the round steel rod is in direct contact with the bushing. The material on the surface bears the pressure from the bushing and enters the yielding state earlier than the material at the center. Then the deformation gradually develops towards the center. This phenomenon verifies the results of the mechanical analysis of the round steel rod in section 5.

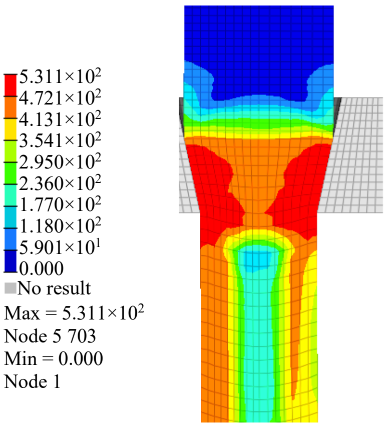

Fig. 13 Distribution of stress(unit: MPa)

6.5 Analysis of parameter influence effect

The constant resistance of the CRYD-TCC is jointly determined by the dimension of the round steel rod and the bushing. The relationship between the cone angle θ, the friction coefficient μ, the cross-sectional shrinkage rate of the round steel rod and the diameter d and the constant resistance of the round steel rod are studied as follows.

6.5.1 Cone angle θ

The cone angle θ is a key structural parameter of the hollow top slab design. By only changing the cone angle while keeping the friction coefficient to be 0.05, the diameter of first section of the round steel rob d to be 10 mm, and the section shrinkage rate to be 30.6%, the constant resistance under different cone angles is calculated and is shown in Fig. 14. It can be seen that as the cone angle increases from 2º to 12º, the constant resistance demonstrates a change of decreasing first and then becoming stabilized. The analysis suggests that the constant resistance is affected by two factors with opposite changing trends as the cone angle increases. They are the height of the second section of the round steel rod and the vertical component of the normal force: (1) As shown in Fig. 15(a), when the cone angle increases, and the round steel rod enters the stable deformation stage, the height of the second rod section decreases, so that the contact area between the round steel rod and the bushing decreases, and the volume of metal involved in plastic deformation also decreases, which results in a rapid decrease in constant resistance. (2) As shown in Fig. 15(b), as the cone angle continued to increase, the vertical component of the normal force on the contact surface between the round steel rod and the bushing increases, but the normal force itself would decrease due to the decrease in the volume of the metal involved in the plastic deformation. Under the action of various changing trends, the constant resistance become stabilized and approaches a constant value. The relationship between constant resistance and cone angle obtained by fitting is

$$F = 34.6\theta^{-0.23} \tag{6}$$

where F is the constant resistance; and θ is the cone angle.

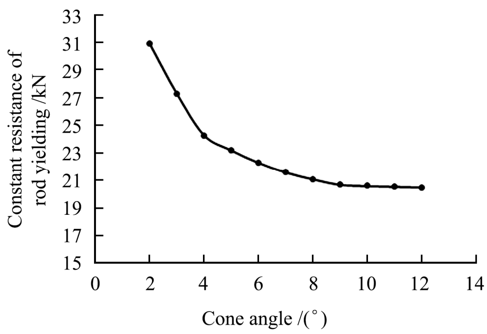

Fig. 14 Relationship between constant resistance and cone angle

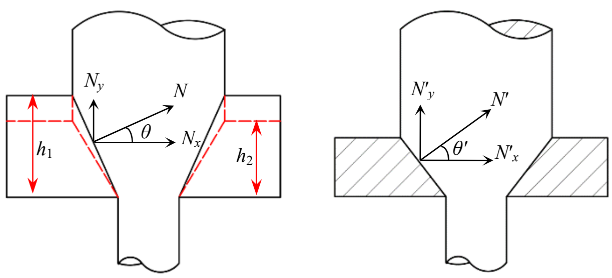

(a) Reduction in height of the second rod section (b) Reduction in vertical component of normal force

Fig. 15 Angle effect

6.5.2 Coefficient of friction μ

In actual engineering use, there is inevitably friction between the round steel rod and the hollow top slab. If the friction coefficient is too large, the round steel rod would be broken in advance. Therefore, it is necessary to analyze the influence of friction between the round steel rod and the hollow top slab on the constant resistance of yielding. By only changing the friction coefficient μ, but keeping the cone angle to be 10º, the diameter d of the round steel rod to be 10 mm, and the section shrinkage rate to be 30.6%, the constant resistance with different friction coefficients is obtained and plotted in Fig. 16. As the friction coefficient increases, the constant resistance increases almost linearly. Since the friction coefficient would increase the constant resistance, this parameter should be used reasonably to increase the utilization rate of the round steel rod material and improve the device performance while ensuring that the round steel rod is not damaged. The linear relationship between constant resistance and friction coefficient obtained by fitting is

$$F = 52.8\mu + 18 \tag{7}$$

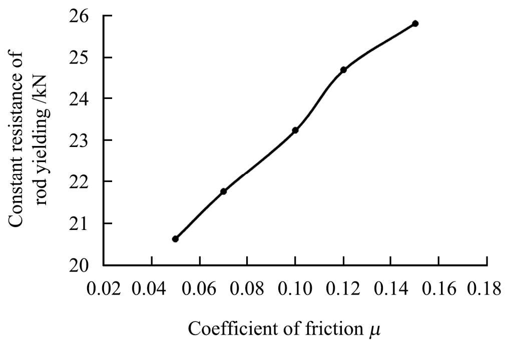

Fig. 16 Relationship between constant resistance and friction coefficient

6.5.3 Section shrinkage rate of round steel rod

By only changing the section shrinkage rate while keeping the diameter d of the round steel rod to be 10 mm, the friction coefficient to be 0.05, and the cone angle to be 10º, the relationship between the constant resistance and the section shrinkage rate is approximately linear, as presented in Fig. 17. Maintaining the cone angle unchanged and increasing the section shrinkage rate would increase the height of the second section of the round steel rod, which increases the volume of the metal involved in plastic deformation and increases the degree of plastic deformation. The linear relationship between constant resistance and area shrinkage is obtained by fitting

$$F = 54x + 4.2 \tag{8}$$

where x is the shrinkage rate (%).

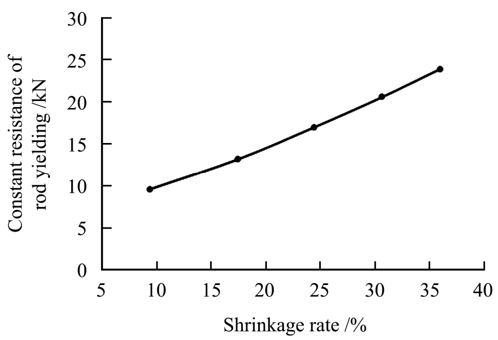

Fig. 17 Relationship between constant resistance strength and rate of shrinkage

6.5.4 Round steel rod diameter d

The diameter d of the round steel rod would be the parameter that affects the constant resistance most intuitively. By only changing the diameter d, while keeping the round steel rod section shrinkage rate to be 17.4%, the cone angle to be 4º, and the friction coefficient to be 0.05. The relationship between the constant resistance and the diameter is obtained as shown in Fig. 18. Given a constant section shrinkage rate, when the diameter increases, the volume of the second section of the round steel rod increases, results in the volume of the metal involved in the plastic deformation increases, so the constant resistance increases approximately linearly. The linear relationship between the constant resistance and the diameter of the round steel rod is obtained by fitting

$$F = 3.7d - 22.7 \tag{9}$$

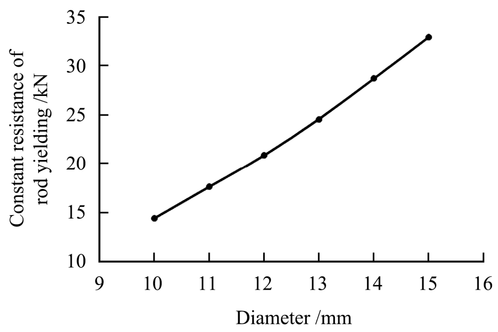

Fig. 18 Relationship between constant resistance and diameter

In summary, it can be concluded that when other parameters remain unchanged, the constant resistance provided by the device is most sensitive to two parameters—the diameter of first section of round steel rod and cone angle, followed by the section shrinkage rate. However, when designing for actual projects, these parameters cannot be changed arbitrarily, because these parameters jointly determine the dimension of the taper hole and the round steel rod, and correlated with each other. For example, when the section shrinkage rate and the diameter of the first rod segment are definite values, the taper angle will determine the length of the second rod segment of the round steel rod. If the cone angle is too small, the second rod segment will be too long to be designed or processed. Therefore, it is necessary to consider various parameters at the same time when designing, and to find the safest combination through a dynamic design approach. Preferably, one should first determine the appropriate height of the second rod segment, that is, the length of the cone mold, and then determine any two parameters among the cone angle, the diameter of the first rod segment, and the area shrinkage rate. By adjusting the third parameter, the constant resistance can be determined. Test and simulation verification should also be carried out before the design size is applied to ensure that the round steel rod will not break.

7 Conclusion

(1) In order to tackle the problem of large rock deformation of tunnelling in squeezing ground, this paper developed a constant resistance yielding device based on the principle of tension-compression conversion, which can be installed at joints of steel arches or sections with large axial forces.

(2) Experiments show that the proposed device presents stable mechanical properties and could provide constant support resistance for tunnels experiencing large extrusion deformation. Two indicators are proposed to measure the performance of the device: the constant resistance and allowable yielding deformation.

(3) Through mechanical analysis, the force characteristics of the round steel rod during plastic shrinkage deformation are obtained as follows: (i) In the critical state of deformation, the round steel rod is subjected to the maximum compressive stress, and the maximum tensile stress at the exit of the taper hole. (ii) The closer to the surface of the round steel rod, the greater the compressive stress and the smaller the tensile stress. The center of the round steel rod at the exit of the taper hole is the most vulnerable to impact.

(4) Through analyzing the characteristics of deformation of the yielding device, four factors that affect the constant resistance provided by the yielding device are summarized as the cone angle, friction coefficient, section shrinkage rate and diameter. The analysis shows that the constant resistance is proportional to the friction coefficient, the area shrinkage rate and the diameter, and as the cone angle increases, the constant resistance is reduced first and then stabilized. These characteristics can be used for different purposes in actual engineering applications. Moreover, understanding these properties provides a theoretical foundation for future designs at different level of details while facilitating better control of the yielding performance of the device.

References

[1] WANG Jian-yu, HU Yuan-fang, LIU Zhi-qiang. High stress soft rock tunnel extrusion deformation and yielding support principle[J]. Modern Tunnelling Technology, 2012, 49(3): 9−17.

[2] KOVÁRI K, AMSTAD C, ANAGNOSTOU G. Design/ construction methods-Tunnelling in swelling rocks[C]// The 29th US Symposium on Rock Mechanics (USRMS). [S. l.]: American Rock Mechanics Association, 1988.

[3] ANAGNOSTOU G, CANTIENI L. Design and analysis of yielding support in squeezing ground[C]//11th ISRM Congress. [S. l.]: International Society for Rock Mechanics and Rock Engineering, 2007.

[4] HOEK E, GUEVARA R. Overcoming squeezing in the Yacambú-Qu ibor Tunnel, Venezuela[J]. Rock Mechanics & Rock Engineering, 2009, 42(2): 389−418.

[5] THUT A, NATEROP D, STEINER P. Tunnelling in squeezing rock—yielding elements and face control[C]//8th International Conference on Tunnel Construction and Underground Structures. Ljubljana: [s. n.], 2006.

[6] SCHUBERT W, MORITZ A B. Controllable ductile support system for tunnels in squeezing rock[J]. Felsbau, 1998, 16(4): 224−227.

[7] HE Man-chao, GUO Zhi-biao. Mechanical property and engineering application of anchor bolt with constant resistance and large deformation[J]. Chinese Journal of Rock Mechanics and Engineering, 2014, 33(7): 1297−1308.

[8] SUN Jun, PAN Xiao-ming, WANG Yong. Study on non-linear rheological mechanical property of squeezing deformation of soft surrounding rock in tunneling and its anchorage mechanism[J]. Tunnel Construction, 2015, 35(10): 969−980.

[9] CHEN Wei-zhong, TIAN Hong-ming, YANG Fu-dong, et al. Study of effects of foam concrete preset deformation layer on long-term stability of deep soft rock tunnel[J]. Rock and Soil Mechanics, 2011, 32(9): 2577−2583.

[10] PAN Yi-shan, XIAO Yong-hui, LI Zhong-hua, et al. Study of tunnel support theory of rock burst in coal mine and its application[J]. Journal of China Coal Society, 2014, 39(2): 222−228.

[11] LEI Sheng-xiang, ZHAO Wei. Study on mechanism of circumferential yielding support for soft rock tunnel with large deformation[J]. Rock and Soil Mechanics, 2020, 41(3): 1039−1047.

[12] TANG Zhi, HAI Dan-feng, PAN Yi-shan, et al. Numerical analysis on energy absorption and anti-impactproperties of mine diameter expanding energy absorption components[J]. Journal of Liaoning Technical University (Natural Science), 2017, 36(3): 310−315.

[13] QIU Wen-ge, WANG Gang, GONG Lun, et al. Research and application of resistance-limiting and energy-dissipating support in large deformation tunnel[J]. Chinese Journal of Rock Mechanics and Engineering, 2018, 37(8): 1785−1795.

[14] BARLA G. Tunnelling under squeezing rock conditions[R]. Innsbruck: Eurosummer-School in Tunnel Mechanics, 2001: 169−268.

[15] KASTNER H. Statik des tunel und stollenbauess[M]. Berlin: Springer-Verlag, 1962.

[16] CHARETTE F, PLOUFFE M. Roofex®–Results of laboratory testing of a new concept of yieldable tendon[C]//Proceedings of the Fourth International Seminar on Deep and High Stress Mining. [S. l.]: Australian Centre for Geomechanics, 2007: 395−404.

[17] VARDEN R, LACHENICHT R, PLAYER J, et al. Development and implementation of the Garford dynamic bolt at the Kanowna Belle Mine[C]//10th underground operators' conference. Launceston, Australia: [s. n.], 2008: 14−16.

[18] WANG G, WU X, JIANG Y, et al. Quasi-static laboratory testing of a new rock bolt for energy-absorbing applications[J]. Tunnelling and Underground Space Technology, 2013, 38: 122−128.

[19] DING Da-jun. Engineering plasticity mechanics[M]. Nanjing: Southeast University Press, 2007.